

第 47 回炉物理夏期セミナー 若手研究会 実施報告書

学生・若手 WG 担当幹事
東北大学 相澤 直人
(株) 東芝 木村 礼

日時：8 月 27 日 (木) 19:30～21:30 (夏期セミナー2 日目)

内容：若手研究者の研究発表

若手研究者として、3 名の学生から自身の研究に関する発表があった。若手研究会においても、初の試みとして夏期セミナーの講義と同様に、研究発表および質疑応答のいずれも全て英語にて開催された。研究発表では、15 分の発表の後、15 分の質疑応答の時間を設けたが、英語にもかかわらず予定時間を上回るほどの活発な議論が交わされた。質疑応答では日本人・海外からの参加者問わず多くの学生が積極的に議論に参加しており、多くの学生が英語での議論を経験出来た大変有意義な研究会となった。

本研究会のプログラムについては以下の通りである。

19:30 ～ 19:35

開会の挨拶 (学生・若手小委員会担当幹事)

19:35 ～ 21:30

研究発表

■ 研究発表者と発表タイトル

「Development of New Statistical Geometry Model using Delta Tracking Method」

名古屋大学 修士課程 2 年 小出 嵩大

(※本発表は 9 月に開催の RPHA15@韓国・済州島にて発表の内容を含む)

「Concept of coated particle fuel LWR with long and high burnup」

東京都市大学 修士課程 1 年 鈴木 高也

(※本発表は 9 月に開催の GLOBAL 2015@フランス・パリにて発表の内容を含む)

「Impact on burnup performance of coated particle fuel design in pebble bed reactor with ROX fuel」

東京工業大学 博士課程 2 年 Ho Hai Quan

Development of New Statistical Geometry Model using the Delta-tracking Method

Takahiro Koide

Nagoya University, Furo-cho, Chikusa-ku Nagoya, Japan, 464-8603

1. Introduction

In the case of neutron transport calculations for typical reactors such as light water reactors or fast breeder reactors, the spatial positions of nuclear fuels are usually known. However, in the case of coated fuel particles in the fuel compact used in very high temperature reactor (VHTR), we should treat a more complicated geometry where fuel particles are randomly distributed in the system. In order to calculate such stochastic geometry using the Monte Carlo method, the statistical geometry model (STGM) has been developed and implemented in the existing Monte Carlo codes [1,2].

In the accident of Fukushima Daiichi Nuclear Power Station, the meltdown of core results in the formation of corium, thus we should expect variety of fuel debris forms in various moderating conditions. Consequently, there are large uncertainties, e.g., the distribution of fuel debris in the system. As one of the possibilities, fuel debris could be randomly distributed in water. It is difficult to rigorously analyze neutronics characteristics for such random geometry, while these random geometry can be effectively treated by the STGM. However, in using STGM, there are some implicit limitations such as fuel particle radius. The applicability and validity of STGM has not been sufficiently discussed. In the present study, we propose a new STGM algorithm using the delta-tracking method to cope the limitation of the traditional STGM model.

2. Delta-Tracking Method

During the random walk of neutron, it is necessary to analysis the neutron collision points. Generally, analysis of collision points is carried out as follows:

1. Search the intersection point of neutron flight path and boundary of nearest neighbor area.
2. Calculate the neutron flight length.
3. Move the neutron to the next boundary area, if the flight length goes over the intersection point of boundary area.
4. The intersection point is assumed as the new emitting point, and then iterate the procedures from 1 to 3.

However, longer calculation time is necessary for flight analysis as the complexity of geometries become increases, such as random distribution of fuel particles in three dimensional geometry.

So, in order to increase computational efficiency of flight analysis, we introduced the delta-tracking method [3,4]. Delta scattering is a non-physical scattering reaction by which energy and flight direction of neutron do not change. Magnitude of the delta scattering cross

section can be set arbitrary. Total cross sections including delta scattering are set to be spatially constant throughout the geometry as follows:

$$\Sigma_{t,g}^* = \Sigma_{t,g}(\vec{r}) + \Sigma_{s,g}^*(\vec{r}) \quad (1)$$

$\Sigma_{t,g}^*$ is a total cross section involving delta scattering in energy group g , $\Sigma_{t,g}(\vec{r})$ is a total cross section in position \vec{r} and energy group g , $\Sigma_{s,g}^*(\vec{r})$ is a delta scattering cross section in position \vec{r} and energy group g .

$\Sigma_{t,g}^*$ is usually set to the maximum value of total cross section throughout the system in the given energy group. By using $\Sigma_{t,g}^*$, total cross section becomes a constant value throughout the system and thus the system can be considered as a homogenized single area such as Fig. 1 from the viewpoint of flight analysis. Consequently, flight analysis can be faster. With the delta-tracking method, flight analysis algorithm of random walk is simplified as follows:

1. Determine the neutron source.
2. Sample the neutron flight length using $\Sigma_{t,g}^*$.
3. Determine the material at reaction point.

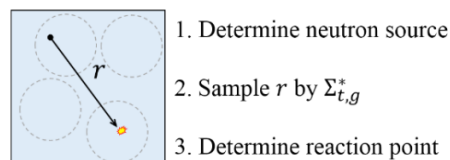


Fig. 1. Determination of collision point utilizing the delta-tracking method.

3. Proposal of New Calculation Model for STGM

On the current STGM model, delta scattering is not used for neutron flight analysis. In the current STGM method, outgoing point of a neutron from a fuel particle is determined at first, then the distance to the nearest fuel particle is sampled by the nearest neighbor distribution (NND), which is the probability distribution of distance between fuel particles. In a fuel particle, ordinary flight analysis is carried out. The advantage of this model is as follows; positions of all of fuel particles are not necessary in advance and collision estimations with these fuel particles are not necessary during flight analysis [1].

On the other hand, all regions are virtually “homogenized” thus outgoing point of a neutron from a fuel particle is not explicitly determined. In such algorithm, direct application of the current STGM method is difficult since the outgoing point of a neutron is not known, thus the nearest neighbor distribution cannot be used. Furthermore, overlapping of fuel particles, which is not physically allowed, is implicitly assumed in the

estimation of NND. Consequently, calculation accuracy becomes worse as the fuel particle radius becomes large, as shown in Fig. 2[5]. In this section, we propose a new STGM algorithm using the delta-tracking method.

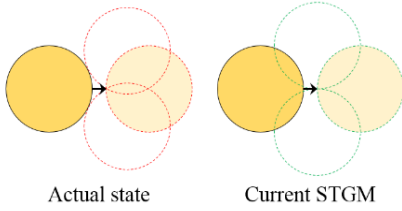


Fig. 2. Interference effect between two fuel spheres: overlapping of fuel particles is implicitly assumed

3.1 Random walk algorithm

In the delta-tracking method, the materials at neutron generation collision points are necessary for flight analysis. In the common delta-tracking calculation, these information is easily known since material spatial distribution is known. However, in the STGM we can sample the material of initial neutron source by using the average packing fraction but not know the explicit material distribution in advance. In order to resolve this issues, the following approaches are used.

3.1.1 Material Assignment at Collision Position

In the average sense, packing fraction can be assumed spatially uniform throughout the calculation system. When the packing fraction is assumed to be spatially uniform, material assignment at collision position is easy, i.e., material (fuel particle or moderator) can be statistically assigned according the packing fraction. However, in reality, the packing fraction has spatial distribution especially the neighbor region of a fuel particle. When many fuel particles with finite radius are randomly distributed, these fuel particles may have physical contact and it causes local fluctuation of the packing fraction near a fuel particle. Thus in the application of STGM this fluctuation should be taken into account.

In order to appropriately treat the fluctuation of the packing fraction, we introduce a radial distribution function of the packing fraction $f_p(r)$. $f_p(r)$ is defined as a volume ratio of fuel to total (fuel + moderator) at distance r . Thus, by using a uniform random number ξ from 0 to 1, it is able to decide material at the collision point as follows:

- $\xi > f_p(r)$: material at collision point is moderator,
- $\xi < f_p(r)$: material at collision point is fuel.

In the present improved model, two different radial distribution functions are necessary depending on the type of neutron generation point as shown in Fig. 3.

- $f_{p1}(r)$: neutron source point is in a fuel particle.

- $f_{p2}(r)$: neutron source point is in moderator.

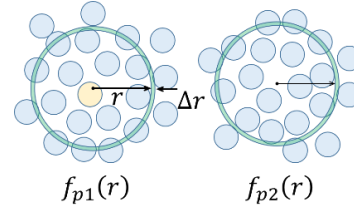


Fig. 3. Radial distribution function of packing fraction.

3.1.2 New STGM Algorithm

The random walk algorithm of neutron using the new STGM algorithm is as follows (Fig.4):

1. Determine a material of the starting point. The starting point on the first batch is decided by the average packing fraction.
2. Sample a flight distance of neutron.
3. Determine a material at the collision point by a flight distance and the radial distribution function of packing fraction. The radial distribution functions are prepared in prior of a STGM calculation.
4. Determine a reaction of neutron by the cross section of determined material. If a fission reaction occurs, this position is set as a new neutron source position.

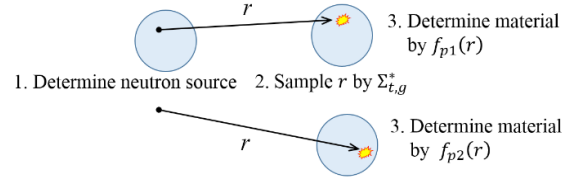


Fig. 4 Neutron random walk in the improved model.

The physical contact of fuel particles that causes fluctuation of the packing fraction is already taken into account in $f_p(r)$. Also, $f_p(r)$ is calculated in systems with random arrangement of fuel particles. Thus, improvement of calculation accuracy and efficiency can be expected compared to the current STGM model.

4. Radial Distribution Function of Packing Fraction

In the present improved STGM model, two radial distribution functions are necessary. In this section, these radial distribution functions are calculated by numerical integration by the Monte Carlo method.

Specifically, an in-house code to calculate an average packing fraction $f_p(r)$ within a distance of r is developed and used. When the Monte Carlo integration is performed from r to $r + \Delta r$, then the packing fraction in this range is expressed as follows:

$$f_p\left(r + \frac{\Delta r}{2}\right) = \frac{1}{N} \sum_{i=1}^N n_i. \quad (2)$$

n_i and N means numbers of samplings at i -th fuel particle within the integral range and all samplings within the integral range, respectively.

The radial distribution functions of packing fraction for the simple cubic lattice (SCL) and 3D random arrangement (RAND) are calculated using the above method. Table I shows calculation condition and Fig. 5 shows calculation procedure. The origin is uniformly sampled. In the case of RAND, fuel particle arrangement is also changed for different initial random seed. As an example, Fig. 6 shows the calculation example of the radial distribution function $f_{p1}(r)$ in the case of average packing fraction is 0.3.

Table I. Calculation condition to estimate radial distribution of packing fraction

N	1000
Δr [cm]	0.01
Number of iteration	1000
Fuel particle radius[cm]	1.0

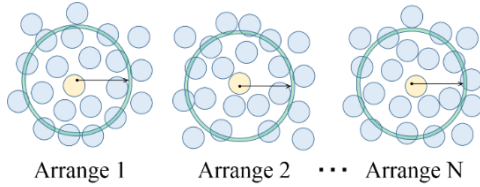


Fig. 5 Calculation procedure of $f_p(r)$.

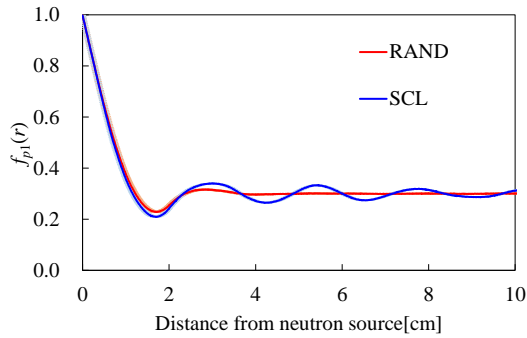


Fig. 6 Distribution function of packing fraction $f_{p1}(r)$.

In the case of SCL, Fig. 6 indicates a periodic structure which is caused by regular and periodic arrangement of fuel particle. These functions converge to the average packing fraction when the sampled flight length is longer than approximately 3cm.

5. Calculation of k-infinity using the conventional and proposed STGM models

In this section, we calculate k-infinity of a system in which fuel particles are randomly distributed in water. The conventional and the present STGM models are used. Calculation conditions are as follows: a number of neutron per batch is 10000, the active number of batches is 1000, number of energy group is 1, and the average packing fraction is 0.1, 0.2, or 0.3, the periodic boundary condition is applied for all boundaries. Verification calculation is carried out in the SCL and RAND. The radial distribution function of packing fraction is used

given by the Monte Carlo integration. Table II shows macroscopic cross sections used in this calculation.

Table II. Macroscopic cross section [cm^{-1}]

	Fuel	Moderator
Σ_a	0.1	0.1
$\nu\Sigma_f$	0.1	0.0
Σ_t	0.1	0.1
Σ_s	0.0	0.0

Figures 7(a) and 7(b) show the calculation result (relative difference from the reference value) of k-infinity for SCL and the RAND. The reference value is calculated at the system where fuel particles are explicitly arranged at 3-dimensional space. In the case of RAND, 1,000 configuration with difference arrangements of fuel particles are prepared, and the mean value of k-infinity calculated from 1,000 configurations is used as the reference value. Number of configurations (1,000) is chosen to sufficiently reduce statistical error for the average value of k-infinity.

The relative difference of k-infinity is calculated as follows:

$$\Delta k_\infty = \frac{k_{calc} - k_{ref}}{k_{ref}} \times 100 [\%] \quad (3)$$

k_{calc} means a value of k-infinity calculated by STGM (the previous or the improved model), k_{ref} means the reference value of k-infinity.

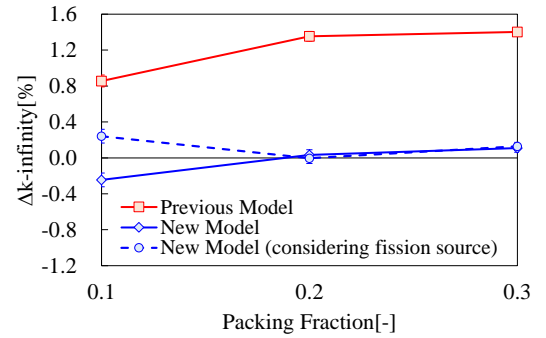


Fig. 7(a). Relative difference of k-infinity (SCL)

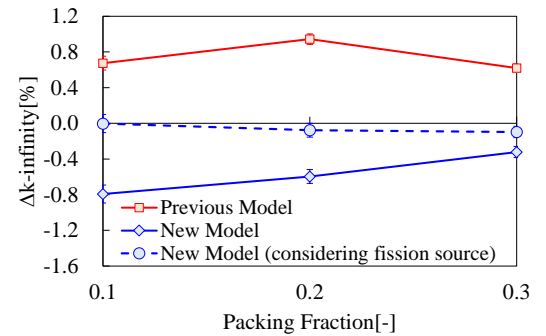


Fig. 7(b). Relative difference of k-infinity (RAND)

As shown in Fig. 7(a), calculation accuracy of proposed STGM model for SCL is better than that of previous STGM model. However, as shown in Fig. 7(b),

calculation accuracy of the proposed STGM model is not significantly improved in RAND.

In the case of RAND, a packing fraction might show spatial fluctuation. Therefore, in the actual Monte Carlo calculation, the fission source distribution may show spatial dependence. For example, location where fuel particles are clouded, higher fission density would be observed. However, in the estimation of packing fraction distribution, this effect is not taken into account.

In order to consider the fission source distribution effect, we calculate the radial distribution function directly from a process of neutron random walk with explicit treatment of random distribution of fuel particles. The distribution function of $f_{p1}(r)$ considering the above effect is calculated with the following calculation conditions: the average packing fraction is 0.3, number of neutrons per batch is 10000, the active number of batches is 1000, and macroscopic cross section is Table II. Estimation result is shown in Fig. 8.

By using $f_{p1}(r)$ considering fission source distribution effect, calculation result of proposed STGM model becomes as a blue broken line. Consequently, it is clarified that calculation accuracy improves by considering fission source distribution. This result suggests that the calculation accuracy and efficiency of proposed STGM will be improved, if the fission source distribution effect can quantitatively estimate before Monte Carlo calculation.

As the result, it is clarified that the improve model can accurately estimate k-infinity of the fuel particle distribution system than the previous STGM model.

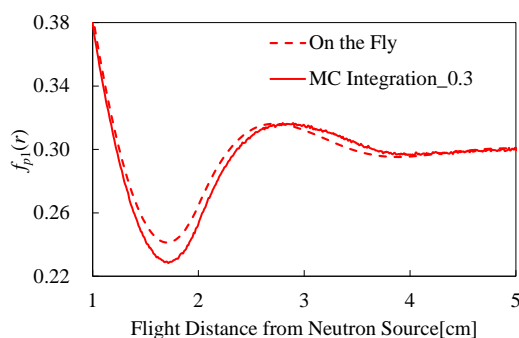


Fig. 8. $f_{p1}(r)$ in consideration of a spatial distribution of fission source.

6. Conclusions

In this study, we developed an improved statistical geometry model with the delta-tracking method. In the previous STGM model, flight analysis of neutron is carried out using the nearest neighbor distribution. In the present study, we simplify the calculation algorithm using the radial distribution function of a packing fraction.

K-infinity obtained by the present improve and previous STGM models are compared with reference value. The calculation results indicate that prediction accuracy of the improved model is higher than that of the previous model.

As a future work, further verifications of the proposed STGM model and consideration of computing time will be carried out.

References

1. Murata I, Takahashi A, et al. "New Sampling Method in Continuous Energy Monte Carlo Calculation for Pebble Bed Reactors," *J. Nucl. Sci. Technol.*, **34**(8), 734 (1997).
2. Nagaya Y, Okumura K, et al. "MVP/GMVP II: General Purpose Monte Carlo Codes for Neutron and Photon Transport Calculations based on Continuous Energy and Multigroup Methods," JAERI 1348, Japan Atomic Energy Research Institute (2005).
3. Ishii K, Maruyama H, "Parallelized Monte Carlo Nuclear Analysis Code VMONT," JAERI-Conf 2000-018, Japan Atomic Energy Research Institute (2000).
4. Jaakko L, "Performance of Woodcock delta-tracking in lattice physics applications using the Serpent Monte Carlo reactor physics burnup calculation code," *Ann. Nucl. Energy*, **37**, pp715-722, (2010).
5. Koide T, Endo T, Yamamoto A, et al. "Impact of Nearest Neighbor Distribution of Fuel Particle on Neutronics Characteristics in Statistical Geometry Model," *Proc. PHYSOR2014*, Kyoto, Japan, Sep. 28-Oct. 2, 2014, (2014). [CD-ROM].

Concept of coated particle fuel LWR with long and high burnup

Takaya SUZUKI

Cooperative Major in Nuclear Energy, Tokyo City University

1. INTRODUCTION

Considering growing nuclear power demand of the world countries, there is a need to enhance the safety of the current light water reactors (LWRs). Safety of nuclear power generation premises a prevention of radioactivity release to the environment. The coated particle fuel LWR (CPF-LWR) employs coated particle fuel for improving the safety. Use of the CPF provides an additional barrier especially for leakage of volatile fission products in the event of cladding failure. Fuel particles are embedded in SiC matrix that forms fuel pellets. Those pellets are clad by usual zircaloy (**Figure 1**). The fuel structure in the cladding entirely different from current pellet fuel. However design parameters of fuel assembly are totally compatible with conventional LWR fuel, so that no modification is necessary to current LWR core design.

The CPF had been originally developed for the use in high temperature gas cooled reactor because it showed excellent retention capability for fission products inside the coating layers at below 1,600°C.

The SiC matrix provides one more barrier between fuel particles and claddings to the dispersion of fission products. Also it maintains relatively low fuel operating temperatures due to the high thermal conductivity of SiC.

Use of the CPF is expected to reduce the risk of radioactivity release, however, the core life is remarkably shortened due to much less initial fissile inventory. The inventory of CPF-LWR using CPF is less than 10% of the present pellet-type fuel with packing fraction (PF)=0.3 which is similar value as high temperature test reactor's (HTTR's) fuel design. To overcome the problem, the fuel composition, the packing fraction of CPF in SiC matrix, and diameter of kernel were optimized through parametric studies.

2. MODELS AND METHOLOGIES

The burnup characteristics of CPF-LWR were analyzed by a unit cell of fuel pin of conventional ABWR. The calculation code used is MVP-BURN which is a burn-up calculation module of MVP which is general purpose monte carlo codes for neutron and photon transport calculations based on continuous energy and multigroup methods. Reference parameters for ABWR are summarized in **Table 1**. The design of the TRISO-type coated particle fuels in Table 1 is the same as that used in HTTR developed by Japan Atomic Energy Agency. For improving burnup characteristics of CPF-LWR, 20% Helium gas

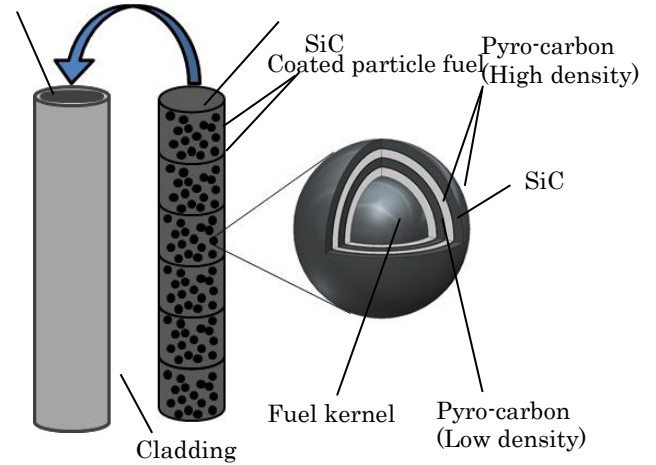


Figure 1 Concept of SiC-coated particle fuel and a fuel rod.

Table 1 Design parameters.

Parameter	Value
Total power(MWt)	3,900
Liner power(Wt/cm)	164
Coolant temperature(°C)	327
Void fraction of coolant (%)	40
Coated particle fuel type	TRISO
Fuel temperature(°C)	627
Pellet radius(cm)	0.96
Fuel pin radius(cm)	1.12
Cladding material	Zircaloy
Clad thickness(cm)	0.071
Fuel pin pitch(cm)	1.44

enriched UO_2 (20% UO_2), depleted uranium- PuO_2 (U-MOX) ThO_2 - PuO_2 (T-MOX) and pure PuO_2 were selected as fuel of CPF-LWR. The plutonium enrichment in U-MOX and T-MOX fuel was set as 30%, 70% and 100%. These fuel materials are loaded in the kernel region of CPF. The compositions of four types of fuels are shown in **Figure 2**. The plutonium composition used in this analysis corresponds to that which is recovered from spent fuel of low-enriched uranium pressurized-water reactor fuel that has released 33MWd/kg fission energy and has been stored for 10 years prior to reprocessing as shown in **Table 2**.

Two kinds of parametric surveys were conducted to evaluate the impacts of PF and kernel diameter on burnup characteristics. The surveyed PF was ranging from 0.3 to 0.05 and kernel diameter was from 600 μ m to 340 μ m. And, heavy metal amounts are equivalent for all cases.

Regarding safety parameters, Doppler coefficient, moderator temperature coefficient and void coefficient were evaluated. In this paper, the core life is defined as duration where the k-infinity (k-inf.) maintains more than unity. In a typical ABWR using 3.5% enriched UO_2 , the

cycle length until refueling is about 400 effective full power days (EFPD) and discharged burnup of three-batch core is 38GWd/t. Evaluated core life and burnup for CPF-LWR were compared to these reference values.

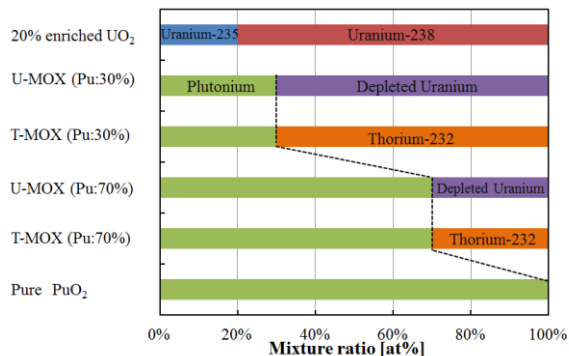


Figure 2 Composition of heavy metal in CPF-LWR fuel.

Table 2 Isotopic composition of plutonium.

Nuclide	Pu-238	Pu-239	Pu-240	Pu-241	Pu-242
wt%	1.3	60.3	24.3	9.1	5.0

3. RESULTS

This chapter described the results for each evaluated subjects about burnup characteristics of CPF-LWR.

3.1. The effect of fuel composition

Figure 3 shows comparison of core life for examined seven types of fuels with PF=0.3. The core life of CPF-LWR using 3.5% enriched UO₂ was only about one month. The core life in case of 20% enriched UO₂, however, was extended to about 400 EFPD. Although the fissile inventories of U-MOX (Pu: 30%) and T-MOX (Pu: 30%) was only about half of that of 20%UO₂, the core lives of two types of MOX (Pu: 30%) fuels were extended to about 500 EFPD. Furthermore, the core lives of U-MOX (Pu: 70%), T-MOX (Pu 70%) and pure PuO₂ were 2-3 times longer than that of the MOX (Pu: 30%).

3.2. The effect of heavy metal amount

3.2.1. Heavy metal amount change by adjusting PF

Figure 4 shows variation of core life by adjusting PF for each fuel composition. The core lives for all cases shortened with decreasing PF. Core lives of 20% UO₂ and two types of MOX (Pu: 30%) fuels with PF<0.3 didn't reach 400 EFPD. The pure PuO₂ with PF=0.3 showed the longest core life of 1,500 EFPD. In spite of the fact that the heavy metal amount in SiC pellets of CPF-LWR was only one third of that of a conventional LWR pellets, the two types of MOX (Pu: 70%) and pure PuO₂ particle fuel could achieve similar or longer core lives.

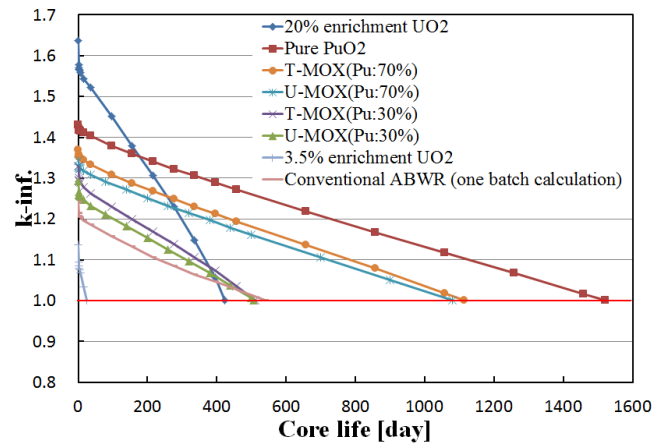


Figure 3 Core lives for various fuels (packing fraction = 0.3).

Figure 5 shows variation of burnup by adjusting PF. All fuel types and PFs examined here showed higher burnup compared to conventional UO₂ pellet. Among them, MOX fuels and pure PuO₂ achieved 3-8 times higher burnup than reference and showed distinctive tendency that the burnup had a maximum value at around PF=0.1-0.2.

This phenomenon can be explained by neutron spectrum softening with decreasing PF. Correlation of PF and neutron flux per unit lethargy for the case of pure PuO₂ is shown in Figure 6. It indicates that the thermal neutron flux was increased with decreasing PF. As a consequence of this trend, the initial reactivity was raised for smaller PF and contributed to the core life extension and burnup enhancement.

Figure 7 shows instant conversion ratio for each fuel type at end of life (EOL). In this study, conversion ratio (CR) was defined as follows;

$$CR = \frac{\sum_c^{Th232} \phi + \sum_c^{U234} \phi + \sum_c^{U238} \phi + \sum_c^{Pu238} \phi + \sum_c^{Pu240} \phi}{\sum_a^{U233} \phi + \sum_a^{U235} \phi + \sum_a^{Pu239} \phi + \sum_a^{Pu241} \phi} \quad (1)$$

where $\sum_c \phi$ in numerator and $\sum_a \phi$ in denominator are generation rate and depletion rate of fissile nuclides, respectively. The CR decreased with decreasing PF. This is why burnup is lower for small PF.

Comparing these two contrary effects on burnup mentioned above, namely reactivity increase by spectrum softening and reduction of instant conversion ratio, the former impact was more dominant.

By reducing PF from 0.1 to 0.05, neutron spectrum is continued to be softened, however, the reactivity cannot be maintained for longer burnup due to less fuel inventory. This is why the burnup has maximum value at around PF=0.1 then decreased in the region of PF<0.1.

3.2.2. Difference in the impact on burnup by adjusting PF and kernel diameter

Figure 8 shows differences on core lives by adjusting PF and kernel diameters of CPF. This research revealed that the differences between adjusting heavy

metal amount of two variation method were small.

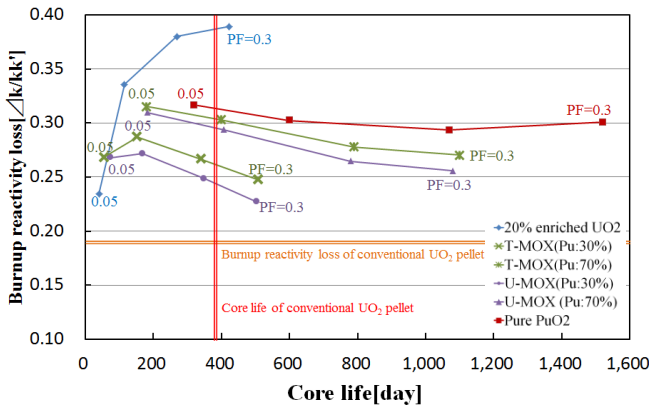


Figure 4 Variation of core life by adjusting PF for each fuel composition.

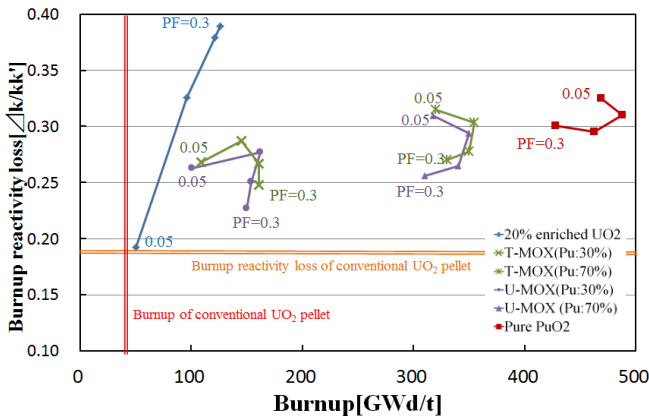


Figure 5 Variation of burnup by adjusting PF for each fuel composition.

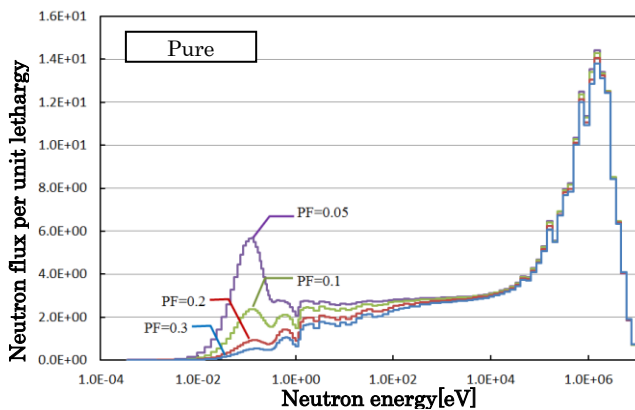


Figure 6 Correlation of the PF and the neutron flux per unit lethargy in pure PuO₂.

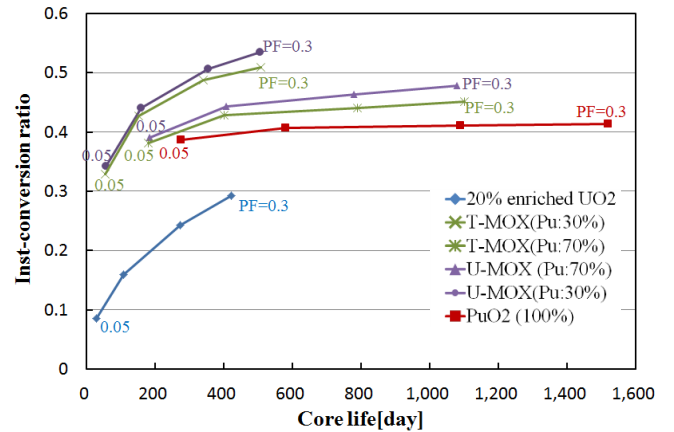


Figure 7 Instant conversion ratios for the each fuel types.

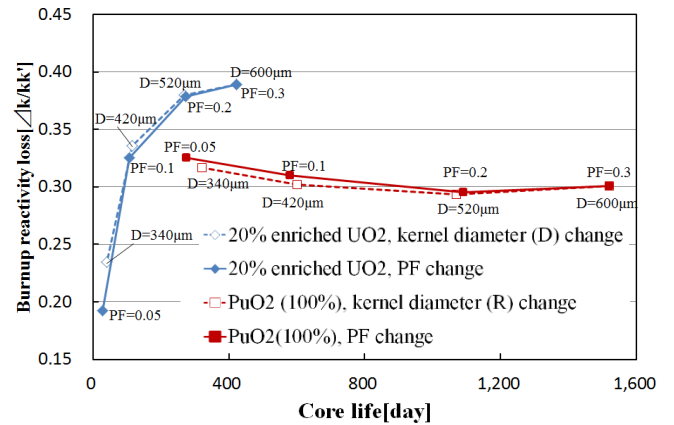


Figure 8 Differences of core life of 20% enriched UO₂ and pure PuO₂ by changing PF and kernel diameter.

3.3. Changes of plutonium consumption rate at EOL by burning of MOX fuels and pure PuO₂

Figure 9 shows Changes of plutonium composition and amount in MOX (Pu: 30%) between beginning of life (BOL) and EOL. In this analysis, PF was fixed at 0.3. The values in Figure 9 are summarized in Table 3. T-MOX (Pu: 30%) had the best plutonium consumption rate of 50%. This rate was 10% higher than that of U-MOX (Pu: 30%). Table 4, 5 show the results for plutonium enrichment 70% and 100%, respectively. Increasing plutonium enrichment of U-MOX and T-MOX, the consumption rate of each fuel exhibited conflicting trends. In U-MOX, the rate increased with increasing the content of plutonium in SiC pellets, but decreased in T-MOX.

This analysis revealed that T-MOX fuel is more beneficial than U-MOX in the effective consumption of plutonium. The principal factor of the gap of plutonium consumption between U-MOX and T-MOX is the differences in the composition rate of Pu-239 at EOL. The rate of Pu-239 in U-MOX at EOL is larger than T-MOX so that U-238 in U-MOX is converted to Pu-239 with burnup. As a result, the consumption rate of T-MOX was larger than that of U-MOX.

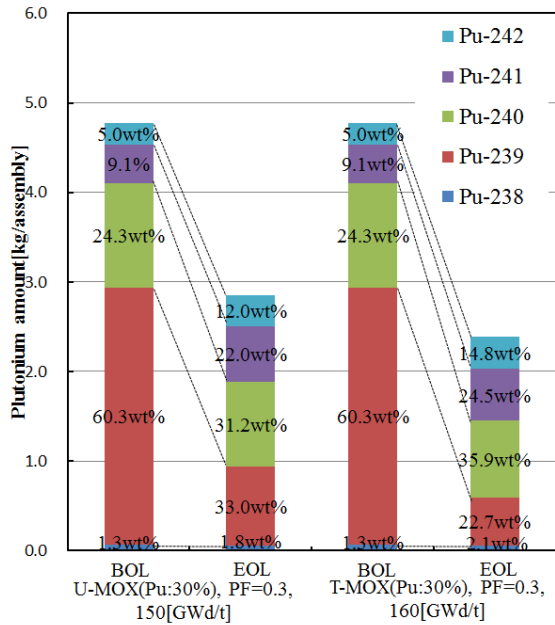


Figure 9 Changes of plutonium composition and amount in MOX (Pu: 30%) between BOL and EOL.

Table 3 Changes of plutonium composition and amount in MOX (Pu: 30%) fuel.

Nuclide	U-MOX (Pu:30%) PF=0.3 150(GWd/t)		T-MOX (Pu:30%) PF=0.3 160(GWd/t)	
	BOL	EOL	BOL	EOL
	Pu-238[wt%]	1.3	1.8	1.3
Pu-239[wt%]	60.3	31.2	60.3	22.7
Pu-240[wt%]	24.3	33.0	24.3	35.9
Pu-241[wt%]	9.1	22.0	9.1	24.5
Pu-242[wt%]	5.0	12.0	5.0	14.8
Plutonium amounts[kg/assembly]	4.8	2.9	4.8	2.4
Consumption rate of Plutonium [%]	40.3		50.0	

Table 4 Changes of plutonium composition and amount in MOX (Pu: 70%) fuel.

Nuclide	U-MOX (Pu:70%) PF=0.3 310(GWd/t)		T-MOX (Pu:70%) PF=0.3 330(GWd/t)	
	BOL	EOL	BOL	EOL
	Pu-238[wt%]	1.3	1.9	1.3
Pu-239[wt%]	60.3	32.9	60.3	28.0
Pu-240[wt%]	24.3	32.6	24.3	34.0
Pu-241[wt%]	9.1	21.9	9.1	23.4
Pu-242[wt%]	5.0	10.7	5.0	12.2
Plutonium amounts[kg/assembly]	11.1	6.3	11.1	5.7
Consumption rate of Plutonium [%]	43.13		48.89	

Table 5 The changes of plutonium composition and amount in pure PuO₂ fuel.

Nuclide	Pure PuO ₂ PF=0.3 428(GWd/t)	
	BOL	EOL
Pu-238[wt%]	1.3	2.7
Pu-239[wt%]	60.3	30.2

Pu-240[wt%]	24.3	34.4
Pu-241[wt%]	9.1	21.5
Pu-242[wt%]	5.0	11.2
Plutonium amounts[kg/assembly]	15.9	8.3
Consumption rate of Plutonium [%]	47.8	

3.4. Reactivity coefficients

Doppler coefficient, moderator temperature coefficient and void coefficient at PF=0.3 were evaluated.

In all of the calculations, reactivity coefficients (RC) are evaluated by taking the difference in k-inf. and dividing by the nominal k-inf., i.e.,

$$RC = \frac{k_{inf,pert} - k_{inf,nom}}{k_{inf,nom} k_{inf,pert}} \quad (2)$$

where $k_{inf,pert}$ is the perturbed k-inf. (e.g., altered temperature of fuel, water conditions, or void fraction) and $k_{inf,nom}$ is the nominal k-inf..

3.4.1. Doppler coefficient

Doppler coefficient was investigated by increasing the water coolant temperature by 20 °C.

Figure 12 shows correlation of Doppler coefficient and plutonium enrichment in the two types of MOX fuels. This analysis revealed that the coefficient of MOX fuel was more negative than that of the conventional UO₂ pellet fuel.

This analysis revealed that Doppler coefficient was degraded with increasing plutonium enrichment.

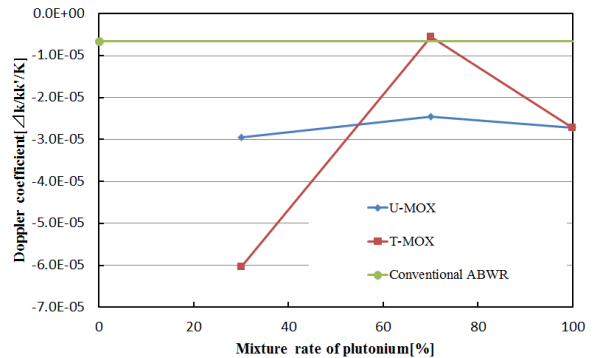


Figure 12 Doppler coefficient and plutonium enrichment.

3.4.2. Moderator temperature coefficient and void coefficient

Moderator temperature coefficient was evaluated by increasing the temperature of the fuel by 20°C, and void coefficient was investigated by raising void fraction in coolant by 5%.

Figure 13 shows plutonium enrichment and moderator temperature coefficient. Void coefficient is shown **Figure 14**. These coefficients showed that the values increased with increasing plutonium enrichment. Through the investigation, it is found that CPF-LWR using U-MOX or T-MOX was negative. However, these coefficients were less negative than conventional UO₂ pellet.

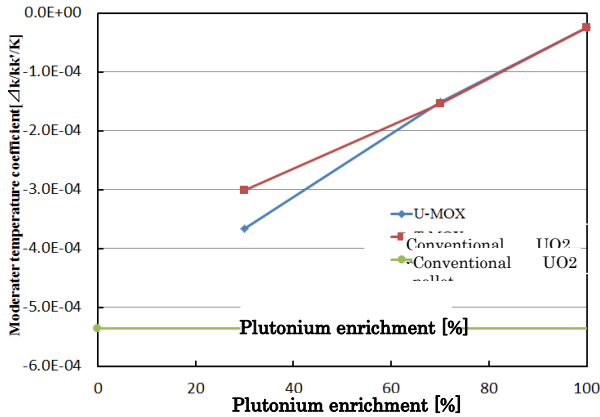


Figure 13 Moderator temperature coefficient and plutonium enrichment.

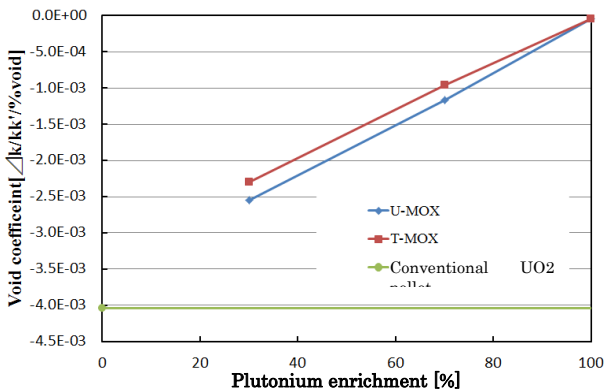


Figure 14 Void coefficient and plutonium enrichment.

4. Conclusions

In this study, the burnup characteristics improvement of CPF-LWR was performed by adjusting fuel composition and design parameters of coated particle fuel. As a result, it was found that CPF-LWR with properly designed particle fuel using MOX fuel or pure PuO₂ fuel showed excellent burnup characteristics. The core life and burnup are extended by 1~4 times and 3~8 times, respectively, than current LWR. Specifically, the fuel specification which achieved the longest core life (1,500EFPD) and the highest burnup (420GWd/t) was pure PuO₂ with PF=0.3. In the case by replacing pure PuO₂ with U-MOX (Pu: 30%) and T-MOX (Pu: 30%), the core lives and burnups exceeded those performances of current, in spite of half of fissile amounts in SiC pellet. Moreover, a core using U-MOX or T-MOX was possible to effectively consume plutonium. Focusing on T-MOX (Pu: 30%) with PF=0.3, it showed that the most superior consumption rate of 50% in this analysis. The value exceeded 10% than the rate of U-MOX (Pu: 30%).

The reactivity coefficients were evaluated about Doppler coefficient, moderator temperature coefficient and void coefficient at PF=0.3. The analysis revealed that evaluated all coefficients are negative. CPF-LWR had almost equivalent reactivity coefficient with the conventional LWR.

CPF-LWR using coated particle MOX fuel is possible to achieve higher burnup and similar core life with conventional pellet type LWR. It also enables effective consumption of plutonium.

However, burnup reactivity loss is slightly larger than that of traditional LWR. To overcome this problem, further optimization of fuel design or use of burnable poison will be considered.

REFERENCE

- [1] M.S. Kazimi, K. R. Czerwinski, M.J. Driscoll, P. Hejzlar and J.E. Meyer, "ON THE USE OF THORIUM IN LIGHT WATER REACTORS", MIT-NFC-TR-016, April 1999
- [2] I. TANIHIRA and Y. SNIMAZU, "Small PWR Using Coated Particle Fuel of Thorium and Plutonium"; Journal of Nuclear Science and Technology, Vol. 44, No. 8, p.1045–1051, 2007
- [3] Rachel A. Shapiro and Matthew J. Vincenzi, "OPTIMIZATION OF FULLY CERAMIC MICRO-ENCAPSULATED FUEL ASSEMBLY FOR PWR", PHYSOR 2014, September 28 - October 3, 2014, on CD-ROM (2014)
- [4] J. Carson Mark¹ with an Appendix by Frank von Hippel² and Edward Lyman, "Explosive Properties of Reactor-Grade Plutonium", Science and Global Security, 17:170–185, 2009
- [5] Akito YAMAMOTO, Tadashi IKEHARA, Takuya ITO and Estsuro SAJI, "Benchmark Problem Suit for reactor Physics Study of LWR Next Generation Fuels", Journal of NUCLEAR SCIENCE and TECHNOLOGY, vol.39, NO.8, p.900-912, August 2002

IMPACT ON BURNUP PERFORMANCE OF COATED PARTICLE FUEL DESIGN IN PEBBLE BED REACTOR WITH ROX FUEL

Hai Quan Ho*

Department of Nuclear Engineering, Tokyo Institute of technology
2-12-1-N1-19, Ookayama, Meguro, Tokyo 152-8550, Japan
Phone: +81-3-5734-2380, Fax: +81-3-5734-2380
Email: quan.h.aa@m.titech.ac.jp

Keywords: reactor design, high temperature gas cooled reactors, pebble bed reactor,
rock like fuel, coated particle fuel

ABSTRACT

The pebble bed reactor (PBR), a kind of high-temperature gas-cooled reactor (HTGR), is expected to be among the next generation of nuclear reactors as it has excellent passive safety features, as well as online refueling and high thermal efficiency. Rock-like oxide (ROX) fuel has been studied at the Japan Atomic Energy Agency (JAEA) as a new once-through type fuel concept. Rock-like oxide used as fuel in a PBR can be expected to achieve high burnup and improve chemical stabilities. In the once-through fuel concept, the main challenge is to achieve as high a burnup as possible without failure of the spent fuel. The purpose of this study was to investigate the impact on burnup performance of different coated fuel particle (CFP) designs in a PBR with ROX fuel. In the study, the AGR-1 Coated Particle design and Deep-Burn Coated Particle design were used to make the burnup performance comparison. Criticality and core burnup calculations were performed by MCPBR code using the JENDL-4.0 library.

Results at equilibrium showed that the two reactors utilizing AGR-1 Coated Particle and Deep-Burn Coated Particle designs could be critical with almost the same multiplication factor k_{eff} . However, the power peaking factor and maximum power per fuel ball in the AGR-1 coated particle design was lower than that of Deep-Burn coated particle design. The AGR-1 design also showed an advantage in fissions per initial fissile atoms (FIFA); the AGR-1 coated particle design produced a higher FIFA than the Deep-Burn coated particle design. These results suggest that the difference in coated particle fuel design can have an effect on the burnup performance in ROX fuel.

1. INTRODUCTION

A pebble bed reactor (PBR) with a once-through-then-out (OTTO) cycle demonstrates many advantages, such as excellent passive safety features, continuous refueling, and high thermal efficiency [1]. Rock-like oxide (ROX) fuel has been studied at the Japan Atomic Energy Agency (JAEA) as a new once-through type fuel concept [2,3,4]. Using rock-like

oxide as fuel in PBRs can be expected to achieve high burnup and improve chemical stabilities. In the once-through fuel concept, the main challenge is to achieve as high a burnup as possible without failure of the spent fuel. To satisfy the high discharged burnup, the PBR with ROX fuel should utilize fuel designs that were successful in high burnup irradiation tests.

Over the past few decades, fuel irradiation tests have been conducted in many countries, including the United Kingdom, Germany, the United States, Japan, and Russia. In experiments, it was found that the AGR-1 [5] and Deep-Burn [6] could achieve high burnup without any observable failures up to approximately 200 GWd/t-HM and 740 GWd/t-HM, respectively.

This study investigated the impact on burnup performance of different coated fuel particles (CFP), comparing the AGR-1 design and Deep-Burn design in a PBR with ROX fuel. The MCPBR [7] code, which was specifically designed for modelling the OTTO cycle movement of PBRs, was used to perform the burnup analysis.

2. OUTLINE OF THE CORE

2.1 Fuel design

Table 1 shows the configuration of the fuel for the AGR-1 and Deep-Burn designs. Both fuel designs have the same fuel pebble geometry. The single-phase YSZ fuel, which consisted of 81.75 mol% YSZ (78.6 mol% $ZrO_2 + 21.4$ mol% $YO_{1.5}$) and 18.25 mol% UO_2 , was used as fuel in the kernel. The kernel diameter of AGR-1 CFP is 50 μm larger than the Deep-Burn CFP, whereas the Deep Burn has a 50- μm thicker buffer layer than AGR-1.

2.2 Reactor design

The schematic view of the reactor core was shown in the **Fig. 1**. The 300 MWt core, 10-m high and 3-m in diameter, was surrounded by a 1-m-thick graphite reflector with a 1-m-high void on top. The pebble packing fraction was 0.61. The total heavy metal loading in a fuel ball was 3 g with 20% of low uranium enrichment. The OTTO cycle was considered for the fuel-loading scheme, in which the core region was separated into 20 horizontal layers and 5 axial flow channels.

2.3 Calculation method

The MCPBR code was used with the JENDL-4.0 library to calculate the burnup of the fuel spheres when they uniformly moved through the core with constant velocity. In MCPBR, a burnup calculation based on a continuous-energy Monte Carlo code, namely MVP-BURN, is coupled with an additional utility code to be able to simulate the OTTO cycle of PBR. The treatment of the OTTO cycle was shown in the **Fig. 2**. The fuel balls in the upper regions progressively move to the next-lower regions, while the top region is refilled by fresh fuel and the balls in the lowest region are directly discharged into the spent fuel tank. The calculation procedure was stopped when reactor core reached the equilibrium condition in which the discharged fuel reached the target burnup of 120 GWd/t-HM. The discharged burnup was set about 120 GWd/t-HM and 112 GWd/t-HM for the AGR-1 reactor and Deep Burn reactor, respectively, to achieve the same k_{eff} at equilibrium condition. Hence, the fuel pebble velocity in AGR-1 reactor was also lower than that in Deep Burn reactor.

3. ANALYSIS RESULTS

3.1 Burnup performance

Table 1

Fuel designs

Properties	AGR-1	Deep Burn
<i>Fuel pebble</i>		
Pebble radius [cm]	3.0	3.0
Thickness of fuel free zone [cm]	0.5	0.5
Density of carbon matrix [g/cm^3]	1.74	1.74
<i>Coated particles</i>		
Kernel diameter [μm]	350	300
Kernel density [g/cm^3]	6.55	6.55
Coating materials	C/C/SiC/C	C/C/SiC/C
Layer thicknesses [μm]	100/40/35/40	150/35/35/40
Layer densities [g/cm^3]	1.10/1.85/3.20/1.85	1.00/1.85/3.20/1.85

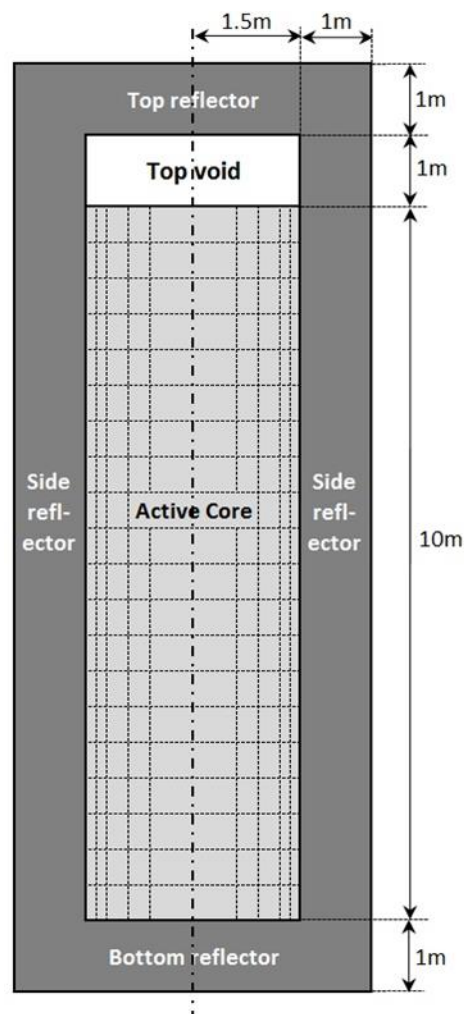


Fig. 1. Reactor geometry

The summarized steady state is shown in **Table 2**. The effective multiplication factors (presented in **Fig. 3**) were a little higher for AGR-1 at the beginning of the cycle, but became identical at the equilibrium state. Because at the initial condition, the total HM loading was the same for both the reactors and the AGR-1 reactor have higher thermal neutron flux than the Deep-Burn reactor. Moreover, the higher thermal neutron flux along with the lower pebble velocity led to

decrease the amount of U-235 in the AGR-1 reactor faster than

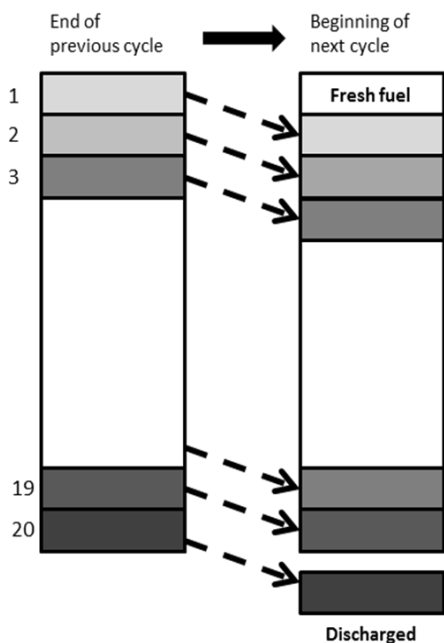


Fig. 2. The OTTO cycle

the Deep-Burn reactor during operation. Therefore, the k_{eff} in the AGR-1 reactor decrease more quickly than in the Deep-Burn reactor and as a result, the k_{eff} became almost the same for both the reactors in the equilibrium condition.

The FIMA for both designs were about 12% corresponding to the discharged burnup of 120 GWd/t-HM. The FIFA decreased from 62.5% to 58.6% by switching the fuel from the AGR-1 design to the Deep-Burn design. The uranium transmutation can be seen more clearly in the Fig. 4. The spent fuel balls were discharged at the bottom of the core, where the amount of remaining U-235 and U-238 of the AGR-1 fuel

Table 2

Burnup performance in equilibrium

Case	AGR-1	Deep Burn
k_{eff}	1.175	1.172
% fissions per initial metal atom (FIMA)	12.50	11.72
% fissions per initial fissile atom (FIFA)	62.50	58.60
Power peaking factor	3.50	3.52
Max. Power per fuel ball [kW]	2.38	3.03

design was smaller than that of the Deep-Burn design. This meant that a larger amount of uranium was burned in the AGR-1 reactor than in the Deep-Burn reactor before discharging.

3.2 Power density and neutron flux comparisons

Fig. 5 shows the power density distribution in the axial and radial directions. In the axial direction, the peak power density in the AGR-1 core was slightly lower than in the Deep-Burn core, resulting in a smaller power peaking factor in the AGR-1 reactor. Moreover, the AGR-1 design gave the lower maximum of total power in a fuel ball than the Deep-Burn design (2.38 kW vs. 3.03 kW). However, the power density in the bottom became larger in the AGR-1 reactor due to the fact that the average power density was the same for both the reactors. In the radial direction, it can be seen that the radial power density profile for the AGR-1 and Deep-Burn designs were almost identical.

The thermal neutron flux ($E < 1.86$ eV) can be observed in Fig. 6. The AGR-1 reactor showed a larger thermal neutron flux than the Deep-Burn reactor due to the difference in kernel diameter. The smaller kernel diameter in the Deep-Burn design enhanced resonance absorption, leading to decreased thermal neutron flux in the Deep-Burn core.

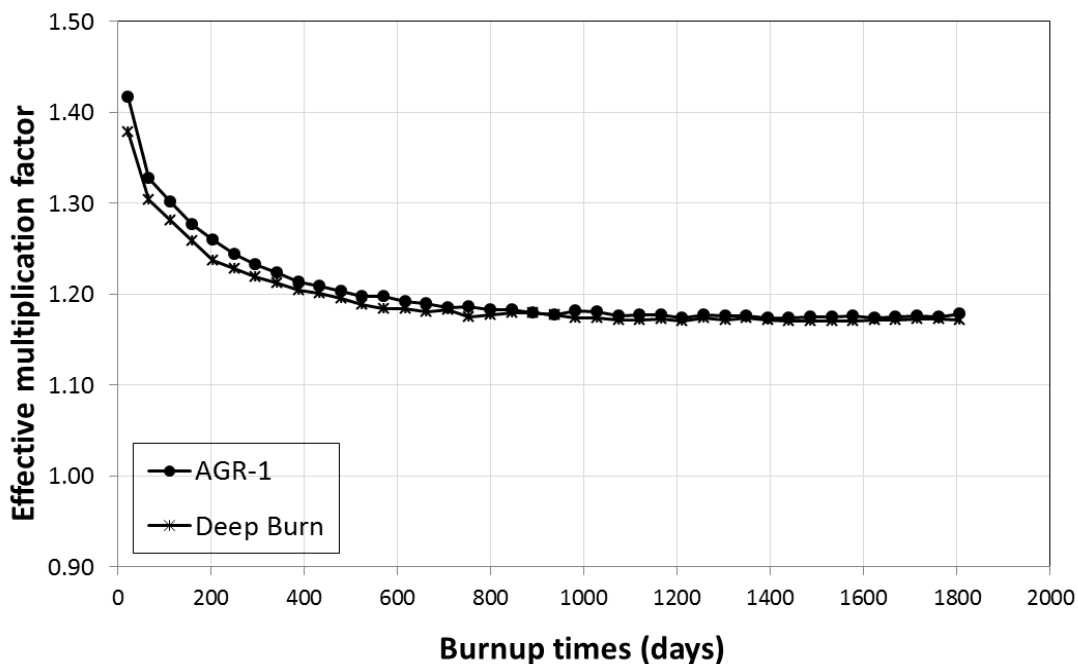


Fig. 3. The effective multiplication factor at equilibrium condition

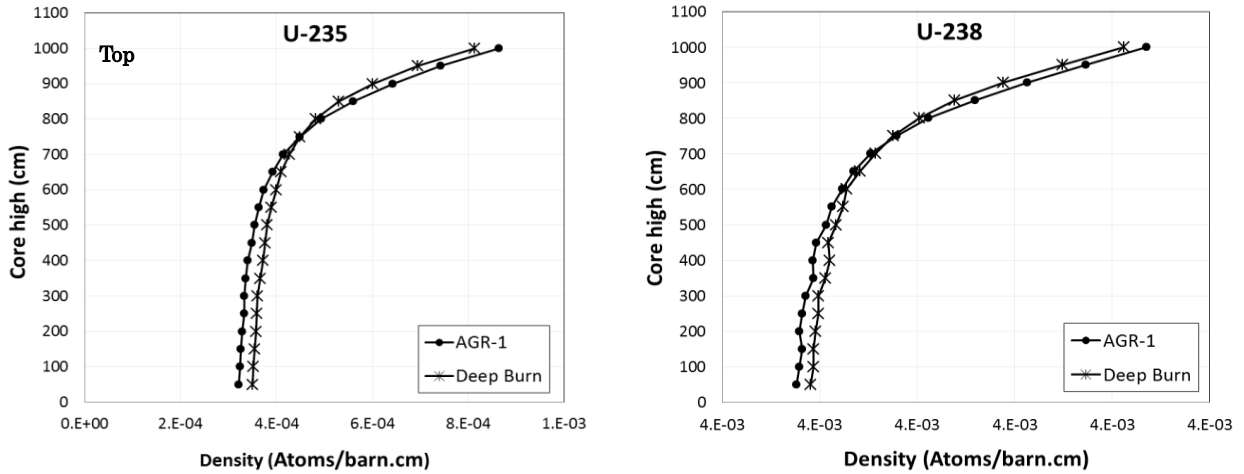


Fig. 4. U-235 and U-238 density distribution at equilibrium condition

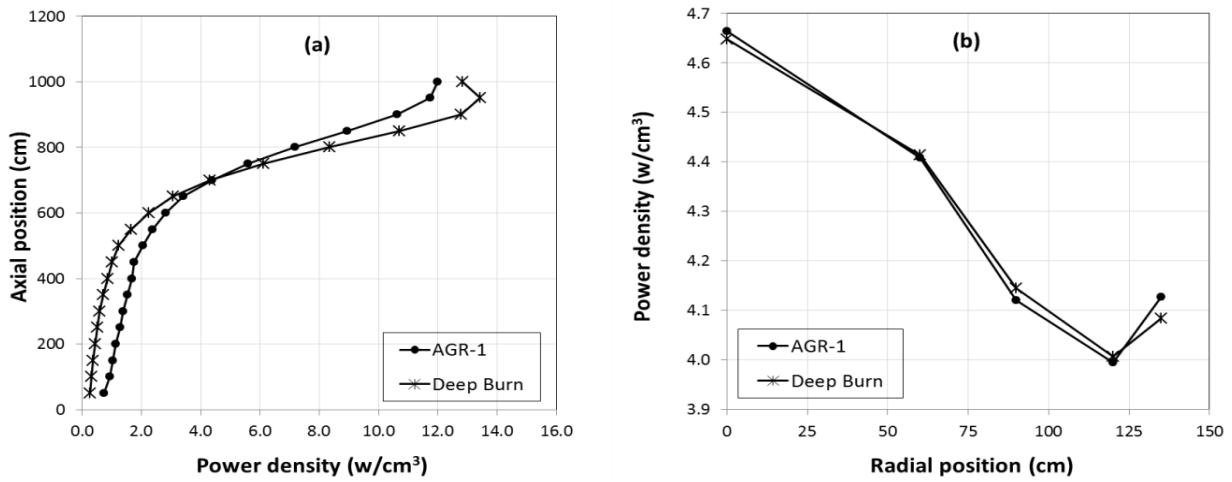


Fig. 5. The power density distribution at equilibrium condition:

(a) axial position, (b) radial position

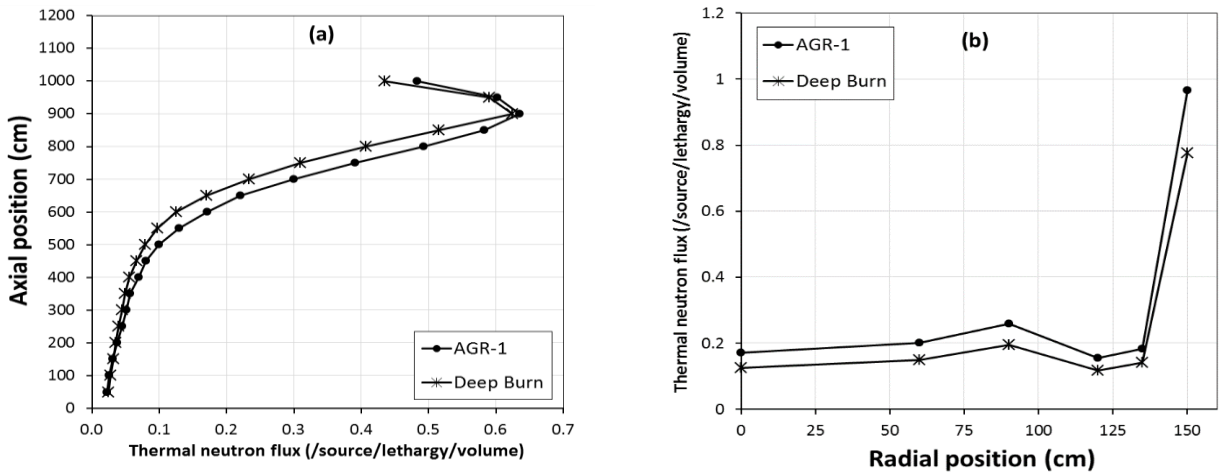


Fig. 6. The thermal neutron flux distribution at equilibrium condition:

(a) axial position, (b) radial position

4. DISCUSSION

The effective multiplication factors k_{eff} were about 1.17 for both the reactor utilizing the AGR-1 design and that using the Deep-Burn design at the equilibrium condition. The maximum

power per fuel ball strongly affected the integrity of the discharged fuel. In this study, the AGR-1 design showed an advantage compared to the Deep-Burn design due to the fact that its 2.38 kW of peak pebble power was lower than the 3.03 kW of the Deep-Burn design.

From the viewpoint of actinides transmutation, with the same k_{eff} at equilibrium state, the AGR-1 design displayed a slightly larger FIFA than the Deep-Burn design 62.5% compared to 58.6%, respectively. This can be explained by the the lower pebble velocity together with thermal neutron flux distribution in Fig. 4: the thermal neutron flux was higher in the AGR-1 core design than in the Deep-Burn core, resulting in more fission reactions occurring in the core with the AGR-1 fuel design.

Regarding the fuel fabrication economy, with the same amount of heavy-metal loading, the amount of AGR-1 CFP in a ball was about 1.5 times smaller than that of the Deep-Burn CFP. For example, 3-g heavy metal loading required approximately 7×10^4 CFPs in a ball for the AGR-1 design in comparison to 11×10^4 CFPs for the Deep-Burn design.

5. CONCLUSIONS

The burnup performance of a PBR with ROX fuel was investigated for both the AGR-1 and Deep-Burn coated fuel particle designs. At equilibrium condition, the reactor with the AGR-1 fuel design showed better behavior than the Deep-Burn fuel design in term of the integrity of discharged fuel, as well as the actinides transmutation. In addition, using the AGR-1 design can reduce the number of CFP fabricated in the fuel matrix by about 1.5 times compared to the Deep-Burn design. These results suggest that the AGR-1 coated fuel particle design should be a candidate for ROX fuel PBRs in further analyses.

REFERENCE

- [1] Andrew C. Kadak, *A future for nuclear energy: pebble bed reactors*, Int. J. of Critical Infrastructures, 2005 Vol.1, No.4,5 pp.330 – 345.
- [2] H. Akie, T. Muromura, H. Takano, S. Matsuura, *A new fuel material for once-through weapons plutonium burning*, Nucl. Technol. 107 (1994) 182 – 189.
- [3] N. Nitani, K. Kuramoto, Y. Nakano, T. Yamashita, Y. Kimura, Y. Nihei, T. Ogawa, *Fuel performance evaluation of rock-like oxide fuels*, Journal of Nuclear Materials 376 (2008) 88-97.
- [4] K. Kuramoto, N. Nitani, T. Yamashita, *Durability test on irradiated rock-like oxide fuels*, Journal of Nuclear Materials 319 (2003) 180 – 187.
- [5] J.T. Maki, *AGR-1 Irradiation Experiment Test Plan*, INL/EXT-05-00593, Rev. 3, October 20, 2009.
- [6] C. Rodriguez, A. Baxter, D. McEachern, M. Fikani, and F. Venneri, *Deep-Burn: making nuclear waste transmutation practical*, Nuclear Engineering and Design, vol. 222 (2003) 299 – 317.
- [7] Topan Setiadipura, Toru Obara, *Development of Monte Carlo-Based pebble bed reactor fuel management code*, Annals of Nuclear Energy 71 (2014) 313-321.